MCB
Journals.ASM.org

Protein Tyrosine Phosphatase-PEST and β8 Integrin Regulate Spatiotemporal Patterns of RhoGDI1 Activation in Migrating Cells

Hye Shin Lee,[a] Mujeeburahiman Cheerathodi,[a] Sankar P. Chaki,[c] Steve B. Reyes,[a] Yanhua Zheng,[b] Zhimin Lu,[b] Helena Paidassi,[f] Celine DerMardirossian,[e] Adam Lacy-Hulbert,[d] Gonzalo M. Rivera,[c] Joseph H. McCarty[a]

Departments of Neurosurgery[a] and Neuro-Oncology,[b] University of Texas M. D. Anderson Cancer Center, Houston, Texas, USA; College of Veterinary Medicine, Texas A&M University, College Station, Texas, USA[c]; The Benaroya Research Institute, Seattle, Washington, USA[d]; Department of Immunology and Microbial Sciences, The Scripps Research Institute, La Jolla, California, USA[e]; Université de Lyon, Lyon, France[f]

Directional cell motility is essential for normal development and physiology, although how motile cells spatiotemporally activate signaling events remains largely unknown. Here, we have characterized an adhesion and signaling unit comprised of protein tyrosine phosphatase (PTP)-PEST and the extracellular matrix (ECM) adhesion receptor β8 integrin that plays essential roles in directional cell motility. β8 integrin and PTP-PEST form protein complexes at the leading edge of migrating cells and balance patterns of Rac1 and Cdc42 signaling by controlling the subcellular localization and phosphorylation status of Rho GDP dissociation inhibitor 1 (RhoGDI1). Translocation of Src-phosphorylated RhoGDI1 to the cell's leading edge promotes local activation of Rac1 and Cdc42, whereas dephosphorylation of RhoGDI1 by integrin-bound PTP-PEST promotes RhoGDI1 release from the membrane and sequestration of inactive Rac1/Cdc42 in the cytoplasm. Collectively, these data reveal a finely tuned regulatory mechanism for controlling signaling events at the leading edge of directionally migrating cells.

The protein tyrosine phosphatase (PTP) family consists of transmembrane and cytoplasmic members that catalyze the dephosphorylation of protein substrates to regulate cell growth, migration, and other processes in development and disease (1, 2). PTPN12/PTP-PEST is a 120-kDa intracellular protein that contains an N-terminal catalytic domain and several proline, glutamate, serine, and threonine (PEST)-rich sequences in the C terminus (3). PTP-PEST is broadly expressed and plays important roles in cell adhesion and migration during development (4, 5). Cultured PTP-PEST$^{-/-}$ cells show impaired motility due, in part, to hyperactivation of the Rho GTPase Rac1 (6). Multiple protein substrates for PTP-PEST have been identified, including Rho guanine nucleotide exchange factors (GEFs) and GTPase activating proteins (GAPs) (7), as well as adhesion proteins, such as paxillin (8), focal adhesion kinase (3, 9), and p120 catenin (10).

Integrins are adhesion receptors for many extracellular matrix (ECM) protein ligands (11). β8 integrin is a 100-kDa glycoprotein that dimerizes exclusively with the 135-kDa αv integrin subunit (12, 13). αvβ8 integrin binds to RGD motifs in various ECM protein ligands, including latent transforming growth factor β (TGFβ) proteins, which are produced by cells as inactive ECM-bound complexes (14). During brain development, αvβ8 integrin in neural cells promotes latent TGFβ activation and signaling to control angiogenesis and formation of the blood-brain barrier (15–20). Single nucleotide polymorphisms in the human β8 integrin (ITGB8) gene that diminish protein expression have been identified in patients with brain vascular malformations (21). ITGB8 expression levels are upregulated in nervous system malignancies, including glioblastoma (22, 23) and peripheral nerve sheath tumors (24).

The β8 cytoplasmic domain is divergent from that in other integrins, suggesting novel signaling functions. For example, β8 integrin lacks NPXY motifs and other conserved amino acid sequences that are common to other integrins and that play key roles in inside-out and outside-in signaling (25, 26). In the developing kidney, β8 integrin has been shown to bind directly to Rho GDP dissociation inhibitor 1 (RhoGDI1) (27), a 21-kDa cytoplasmic protein that inhibits activation of Rho GTPases (28). RhoGDIs suppress Rho GTPase signaling by sequestering GDP-bound proteins in the cytoplasm and inhibiting conversion to the active GTP-bound forms (29, 30). In migrating cells, growth factors stimulate Src-mediated phosphorylation of RhoGDI1 on Y156, and this phosphorylation diminishes RhoGDI1 affinities for GDP-bound cytoplasmic Rho GTPases and promotes their activation at the membrane (31). Paradoxically, phosphorylated RhoGDIs also translocate to the cell's leading edge, although the functional importance of these events has remained uncertain. In addition, proteins that interact with phosphorylated RhoGDIs and mediate their dephosphorylation and release from the leading edge have remained enigmatic. Here, we report on a protein complex consisting of αvβ8 integrin and PTP-PEST that controls RhoGDI1 activities by regulating its subcellular localization and phosphorylation status. Hence, the αvβ8 integrin-PTP-PEST-RhoGDI1 multimeric protein complex serves to fine-tune Rac1 and Cdc42 signaling at the leading edge to drive directional cell migration.

Received 29 January 2015 **Accepted** 29 January 2015

Accepted manuscript posted online 9 February 2015

Citation Lee HS, Cheerathodi M, Chaki SP, Reyes SB, Zheng Y, Lu Z, Paidassi H, DerMardirossian C, Lacy-Hulbert A, Rivera GM, McCarty JH. 2015. Protein tyrosine phosphatase-PEST and β8 integrin regulate spatiotemporal patterns of RhoGDI1 activation in migrating cells. Mol Cell Biol 35:1401–1413. doi:10.1128/MCB.00112-15.

Address correspondence to Joseph H. McCarty, jhmccarty@mdanderson.org.

Supplemental material for this article may be found at http://dx.doi.org/10.1128/MCB.00112-15.

doi:10.1128/MCB.00112-15

MATERIALS AND METHODS

Isolation and manipulation of mouse astrocytes and fibroblasts. All experimental animal procedures were reviewed and approved by the Institutional Animal Care and Use Committee at the University of Texas M. D. Anderson Cancer Center. Astrocytes were cultured from the cerebral cortices of wild-type or $\beta8^{-/-}$ newborn pups and propagated on laminin-coated dishes, as described previously (32). Given the limited growth of primary astrocytes in culture, we immortalized cells as described previously (33). Primary astrocytes were transduced with retroviruses expressing E6/E7 and V12–H-Ras oncogenes, and cells were selected in growth medium containing 0.5 μg/ml puromycin and 750 μg/ml G418. Cell migration in scratch-wound assays was imaged by time-lapse microscopy using an Olympus IX81 inverted microscope mounted with an automated stage, humidified chamber, and DP25 digital camera. SlideBook software (Intelligent Imaging Innovations) was used to quantify the migration index. Migration was analyzed in separate frames, and wound closure was defined when five migrating cells from opposite sides of the scratch (within a ×200 magnification field) made contacts within the wound region. For analyzing integrin protein localization, $\beta8^{-/-}$ astrocytes were infected with retroviruses expressing green fluorescent protein (GFP) or β8-GFP, and cells were plated on laminin-coated dishes. The GFP-tagged integrin construct was generated by ligating a GFP cDNA into the retroviral plasmid pQCXIP (Clontech) via NotI and BamHI restriction sites. A cDNA encoding full-length murine β8 integrin was inserted upstream of GFP using the NotI and AgeI restriction enzyme sites.

Control and PTP-PEST-null mouse embryonic fibroblasts (MEFs) have been described elsewhere (6) and were provided by one of us (Zhimin Lu). MEFs were transiently transfected with a pcDNA3 expression vector containing a constitutively active (Y527F mutant) chicken Src cDNA originally purchased from Addgene (plasmid 13660) in combination with RhoGDI1-myc or Flag-tagged PTP-PEST. Experiments were performed in the absence of pervanadate.

Immunoprecipitation, immunoblotting, and antibodies. Cells were surface biotinylated in phosphate-buffered saline (PBS) containing 0.1 mg/ml normal human serum-biotin (Pierce Chemicals, Inc.), rinsed with Tris-buffered saline, and lysed in radioimmunoprecipitation assay (RIPA) buffer (10 mM Tris, pH 7.4, 1% NP-40, 0.5% deoxycholate, 0.1% SDS, 150 mM NaCl, 1 mM EDTA) with protease and phosphatase inhibitors (Roche). Protein concentrations were determined using a bicinchoninic acid (BCA) assay kit (Thermo Scientific). Membranes were probed with streptavidin-horseradish peroxidase (HRP) and chemiluminescent reagents (Amersham). The following antibodies were purchased: rabbit anti-phospho-Src (Y416), rabbit anti-phospho-Src (Y527), mouse anti-Src, rabbit antidoublecortin, rabbit anti-Erk1/2, mouse anti-PTP-PEST, and rabbit anti-Cdc42 (Cell Signaling Technology); rabbit anti-RhoGDI and mouse anti-phosphotyrosine pY99 (Santa Cruz Biotechnology); mouse anti-myc and anti-V5 antibodies (Invitrogen); mouse anti-Flag (M2) antibody and phalloidin-tetramethyl rhodamine isocyanate (Sigma); rabbit and mouse anti-GFP antibodies (Abcam); and mouse anti-Rac1 and mouse anti-N-cadherin antibodies (BD Bioscience). The antibody recognizing phosphoserines 198 and 203 in mouse Pak1 has been described previously (34). HRP- or Alexa Fluor-conjugated secondary antibodies were purchased from Jackson ImmunoResearch. Details about the anti-β8 and anti-αv integrin antibodies used for immunoprecipitation and immunoblotting have been reported previously (17, 35).

Generation of GST fusion proteins and deletion constructs. A cDNA encoding the entire 67-amino-acid sequence of the human β8 integrin cytoplasmic tail (β8cyto) was inserted in the pGEX-6P-1 bacterial expression vector. Alternatively, pGEX-6P-1 vectors engineered to express different PTP-PEST catalytic domain proteins (wild-type or C231S or D199A mutant proteins) were used to transform BL21(DE3) bacteria. Cultures in log-phase growth were treated with IPTG (isopropyl-β-D-thiogalactopyranoside; 1 mM), and glutathione *S*-transferase (GST)-tagged proteins were purified from detergent-soluble lysates using glutathione-agarose (Pierce). The RhoGDI1 C-terminal domain (CTD) construct was generated by amplifying cDNA sequences encoding amino acids 74 to 204 of human RhoGDI1 and subcloning the fragment into the XhoI/BamHI sites of pcDNA3.1-Myc. The cDNA sequences encoding the N-terminal domain (NTD; amino acids 1 to 300) or the CTD (amino acids 301 to 780) of human PTP-PEST were amplified by PCR using full-length pcDNA3-Flag-PTP-PEST as a template. Fragments were subcloned into the BamHI/NotI sites of pcDNA3-Flag. GST-PTP-PEST catalytic domain constructs (wild-type and C231S mutant constructs) were provided by Sarita Sastry and have been described elsewhere (10). The PTP-PEST D199A mutation was generated by QuikChange site-directed mutagenesis (Agilent) using the wild-type construct as a template. The mutagenesis primers used to generate the D199A mutation were (5′-GTTTCATTATGTGAACTGGCCAGCCCATGATGTTCCTTCATCATTTG-3′ (forward) and 5′-CAAATGATGAAGGAACATCATGGGCTGGCCAGTTCACATAATGAAAC-3′ (reverse). The D199A point mutation was confirmed by DNA sequencing (Lone Star Labs).

Subcellular fractionation and phosphatase assays. Cells were lysed in fractionation buffer (10 mM Tris, pH 7.5, 5 mM $MgCl_2$, 1 mM dithiothreitol, 0.25 M sucrose) containing phosphatase and proteinase inhibitor cocktails, and membrane/cytosol fractions were isolated by ultracentrifugation. To assay PTP-PEST activities *in vitro*, 1 μg GST-RhoGDI1 protein (Cytoskeleton, Inc.) was phosphorylated *in vitro* by mixing with 10 units purified p60-Src (Millipore) and kinase buffer containing 100 μM ATP for 60 min at 30°C. GST-RhoGDI1 was fractionated using glutathione-agarose and then incubated with various amounts of the PTP-PEST catalytic domain (AnaSpec) for 2 h at 30°C. Proteins were resolved by SDS-PAGE and immunoblotted for phosphorylated tyrosine or GST. Controls were p60-Src protein alone or GST-RhoGDI1 alone in the absence of PTP-PEST.

FRET and TIRF imaging. The Raichu-Cdc42 and Raichu-Rac1 intramolecular fluorescence resonance energy transfer (FRET) biosensors have been described previously (36). Mouse astrocytes were cultured on fibronectin-coated (10 μg/ml) glass-bottom MatTek dishes in low-glucose Dulbecco modified Eagle medium. Cells were transfected with plasmids carrying Cdc42 or Rac1 FRET probes. After 24 h the cells were washed and FRET imaging was performed using a Zeiss Stallion microscope configured with cyan fluorescent protein (CFP)-yellow fluorescent protein (YFP) FRET module using a 63× (numerical aperture, 1.40) oil objective. Time-lapse images (CFP, FRET, and YFP) were taken every 1 min for 30 to 60 min. Images were analyzed using EMBL ImageJ software. A binary mask was derived from the YFP image and multiplied by the CFP and FRET images separately. Subsequently, FRET images were divided by CFP images to obtain FRET/CFP ratios. A rainbow 2-color lookup table was applied, and brightness and contrast were adjusted to display the ratio of FRET images in an intensity-modulated manner. For quantitative analysis, YFP-masked FRET and CFP images were thresholded to measure the pixel intensity of each individual image in the stack, and FRET/CFP intensity ratios were calculated as previously reported (37). Line scans were generated using ImageJ to visualize the gradient of FRET activity across the cell as described previously (38, 39).

To visualize Cdc42 and Rac1 activation at the plasma membrane by total internal-reflection fluorescence (TIRF), cells were transfected with the GFP-wGBD (where wGBD is the Cdc42-binding domain of N-WASP) (40) or pYpet-Pak binding domain (pYpet-PBD) (41) reporter, respectively. Imaging was performed with a TIRF 3 microscope (Carl Zeiss Microimaging, Thornwood, NY) equipped a with Photometrics Quant EM 512SC electron-multiplying charge-coupled device. Time-lapse images were obtained every 15 s for 30 to 60 min using a Plan-Apochromat 100× (numerical aperture, 1.46) oil objective lens. In both FRET and TIRF experiments, time-lapse series from 3 to 5 individual cells were obtained in single replicates and experiments were repeated three times. FRET and TIRF quantitative data were analyzed by one-way analysis of variance (Minitab 16) and displayed using box plot representations. Differences were considered significant at P values of ≤ 0.05.

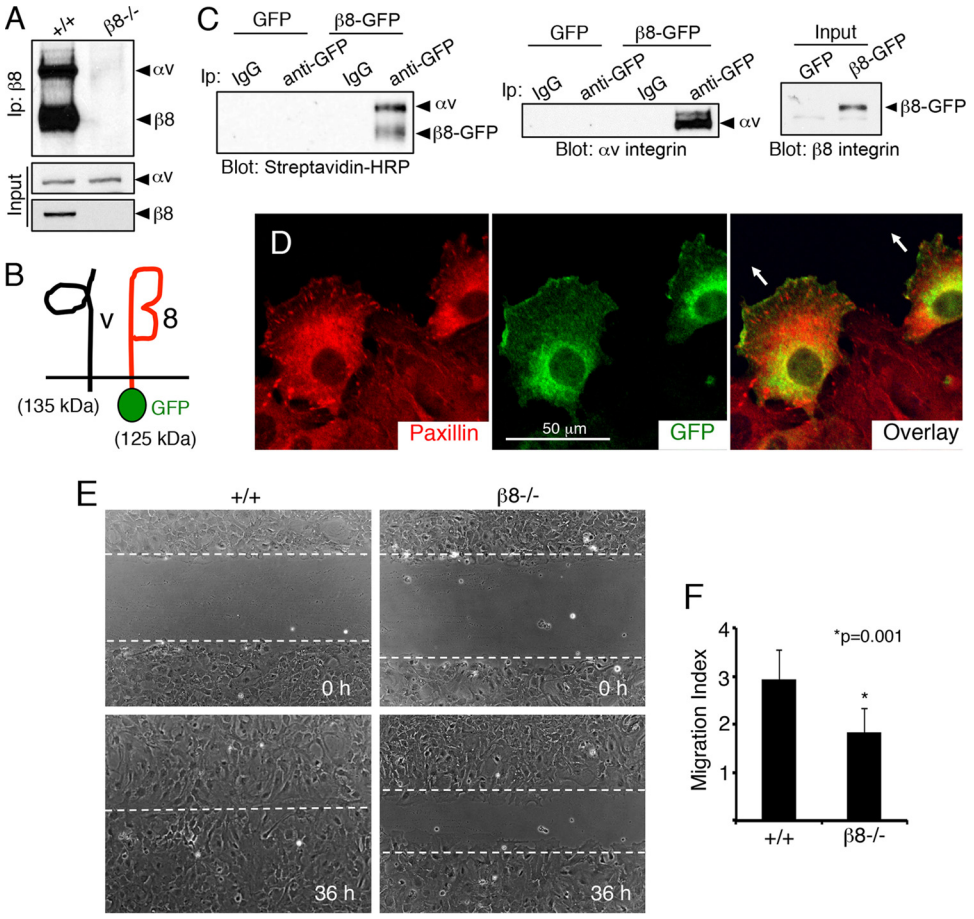

FIG 1 β8 integrin promotes directional cell migration *in vitro*. (A) αvβ8 integrin is expressed in primary astrocytes. Biotinylation and immunoprecipitation (Ip) with an anti-β8 integrin antibody revealed cell surface integrin protein expression in wild-type (+/+) cells and a complete absence of αvβ8 integrin dimers in $\beta8^{-/-}$ cells. Inputs show that αv integrin is expressed in the absence of β8 gene expression. (B) Schematic showing an engineered 125-kDa protein comprised of GFP fused to the C terminus of mouse β8 integrin which dimerizes with the 135-kDa αv integrin subunit. (C) Astrocytes expressing GFP or β8-GFP were cell surface biotinylated and immunoprecipitated with control IgG antibodies or anti-GFP antibodies and then labeled with streptavidin-HRP. Note that β8-GFP forms cell surface complexes with αv integrin (left). Astrocytes expressing GFP or β8-GFP were lysed and immunoprecipitated with anti-GFP and immunoblotted with anti-αv integrin (right). (D) Confluent monolayers of astrocytes infected with lentiviruses expressing β8-GFP protein were scratched and then immunolabeled with antipaxillin (left) and anti-GFP (middle), revealing that β8-GFP is enriched at the leading edge of migrating cells (overlay, right). Arrows in the right panel indicate the direction of migration. (E) Confluent monolayers of wild-type and $\beta8^{-/-}$ astrocytes were scratched, and directional cell migration was imaged over 36 h. (F) Quantitation of integrin-dependent migration defects in scratch-wound assays.

Experimental mice. $\beta8^{flox/flox}$ and $\beta8^{+/-}$ mice were purchased from the Mutant Mouse Regional Resource Center. Nestin-Cre (N-Cre) transgenic mice (42) were purchased from The Jackson Laboratory. To generate control and conditional knockout mice, $\beta8^{flox/flox}$ females were bred with hemizygous nestin-Cre (N-Cre/+) transgenic males. The genotypes of the F1 progeny were determined by PCR-based amplification of genomic DNA isolated from ear snips (20). N-Cre/+; $\beta8^{flox/+}$ males were then crossed with $\beta8^{flox/flox}$ females. Controls (N-Cre/+; $\beta8^{flox/+}$ mice) were heterozygous null for β8 integrin gene expression in cells that express Cre, whereas mutant littermates (N-Cre/+; $\beta8^{flox/flox}$ mice) were homozygous null for β8 integrin gene expression in Cre-expressing cells. $Tgfbr2^{flox/flox}$ mice (43) were crossed to nestin-Cre transgenic mice as described previously (19). Bacterial artificial chromosome (BAC) doublecortin-GFP (DCX-GFP) mice (44) were purchased from the Mutant Mouse Regional Resource Center.

SVZ isolation and migration assays. Mouse subventricular zone (SVZ) regions were dissected as described previously (35). Dasatinib (1 μM; Bristol-Myers), PTP-PEST inhibitor (10 μM; EMD Millipore), or NSC23766 (50 to 100 μM; R&D Systems) was added to Matrigel as well as culture medium for the entire culture period. Each explant was imaged under an inverted light microscope (Olympus), and the mean migration distance was calculated by measuring the length of the neuroblast chains from the edge of each explant using ImageJ software. At least 5 individual explants were analyzed in each experimental group. For immunoblotting, cell lysates were prepared in RIPA buffer, and protein concentrations were determined using the BCA assay (Thermo Scientific). Alternatively, after cardiac perfusion with 4% paraformaldehyde–PBS, brains were removed and SVZ/rostral migratory stream (RMS) regions were dissected and postfixed. Tissue slices (100 to 200 μm) were prepared with a vibratome, and immunofluorescence was imaged with a Zeiss LSM 510 confocal microscope. For *in vitro* scratch-wound assays, Smartpool small interfering RNAs (siRNAs; Thermo Scientific) were used to silence PTP-PEST.

RESULTS

αvβ8 integrin promotes directional cell migration. To analyze the roles for β8 integrin-dependent signal transduction in directional cell motility, we cultured brain astrocytes from wild-type and $\beta8^{-/-}$ mice. Biotinylation and immunoprecipitation experiments revealed that wild-type astrocytes express robust levels of

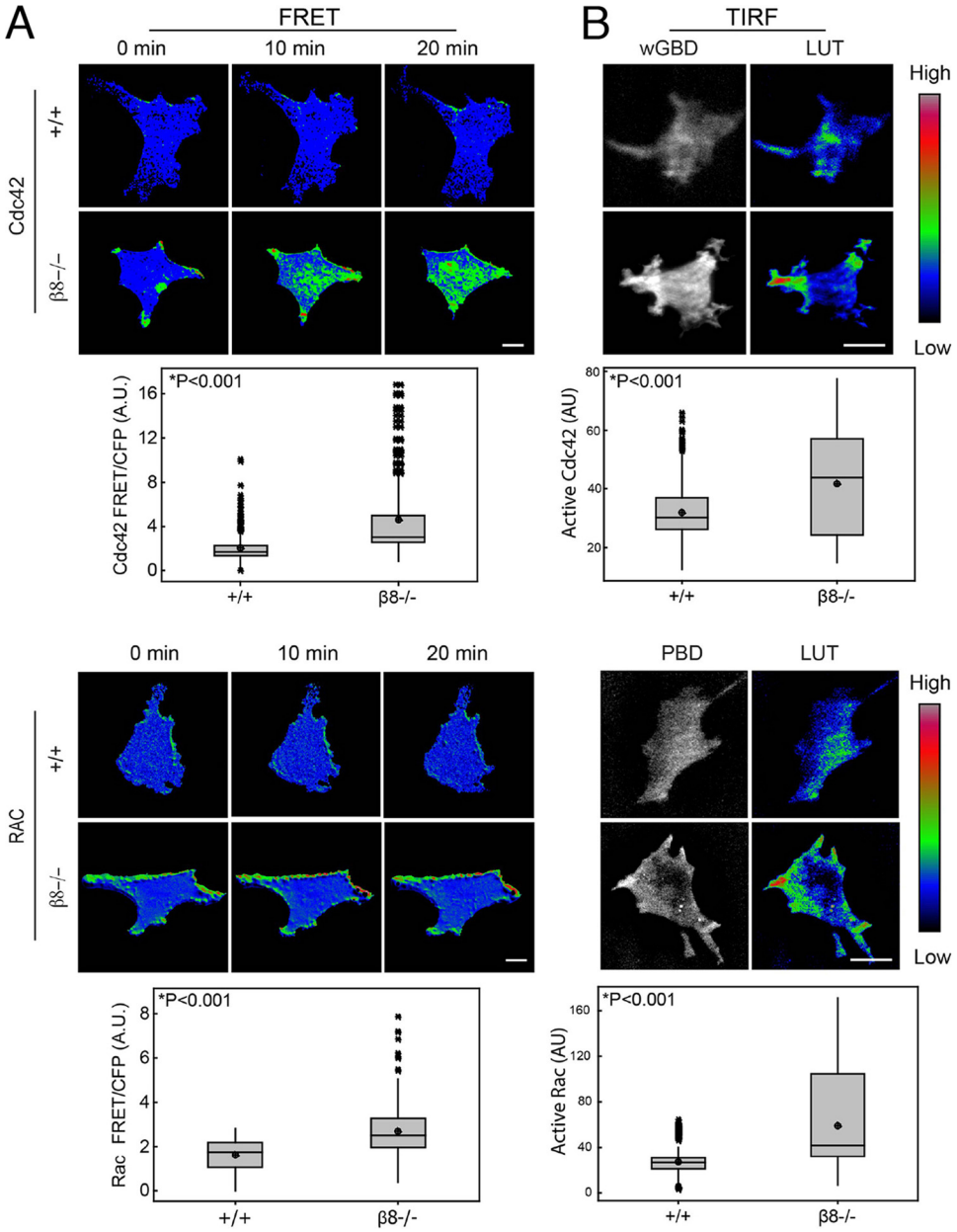

FIG 2 β8 integrin dampens Rac1 and Cdc42 activation in live cells. (A) FRET images of wild-type (+/+) and $\beta8^{-/-}$ astrocytes expressing Raichu-Cdc42 (top) or Raichu-Rac (bottom). The images shown were selected at particular intervals from the beginning of a time-lapse series. (B) TIRF images of wild-type and $\beta8^{-/-}$ astrocytes expressing EGFP-wGBD (top) or pYpet (bottom), Cdc42 and Rac biosensors, respectively, that are sensitive to RhoGDIs. Note that $\beta8^{-/-}$ astrocytes displayed increased and mislocalized activation of Cdc42 and Rac1. Quantitative analysis was based on time-lapse series collected from 3 to 5 cells of each genotype in each of three independent experiments. Each time-lapse series consisted of 30 to 60 frames. Data are presented in box-and-whiskers diagrams, where the bold central lines of the box plots indicate the median values, whereas the top and bottom lines indicate the 3rd and 1st quartiles, respectively. The whiskers extend up to 1.5 times the interquartile range. Statistically significant differences between genotypes are indicated. LUT, lookup table; A.U., absorbance units.

αvβ8 integrin protein on the cell surface, whereas αvβ8 integrin heterodimers were not detected in $\beta8^{-/-}$ cells owing to itgb8 ablation (Fig. 1A). Subcellular localization of αvβ8 integrin protein expression was determined by infecting $\beta8^{-/-}$ cells with a retrovirus expressing full-length murine β8 integrin fused at the C terminus to GFP (β8-GFP) (Fig. 1B). Cell surface expression and dimerization of β8-GFP with endogenous αv integrin protein were confirmed by biotinylation and immunoprecipitation (Fig. 1C). The αvβ8-GFP fusion protein was enriched at the leading edge of migrating cells but not in paxillin-expressing focal adhesions (Fig. 1D; see also Fig. S1A in the supplemental material). Next, β8 integrin-dependent directional migration was quantified in wild-type and $\beta8^{-/-}$ cells using live-cell imaging and scratch-wound assays (45). Integrin-dependent differences in early stages of cell polarity were not detected (data not shown). However, $\beta8^{-/-}$ cells displayed defects in sus-

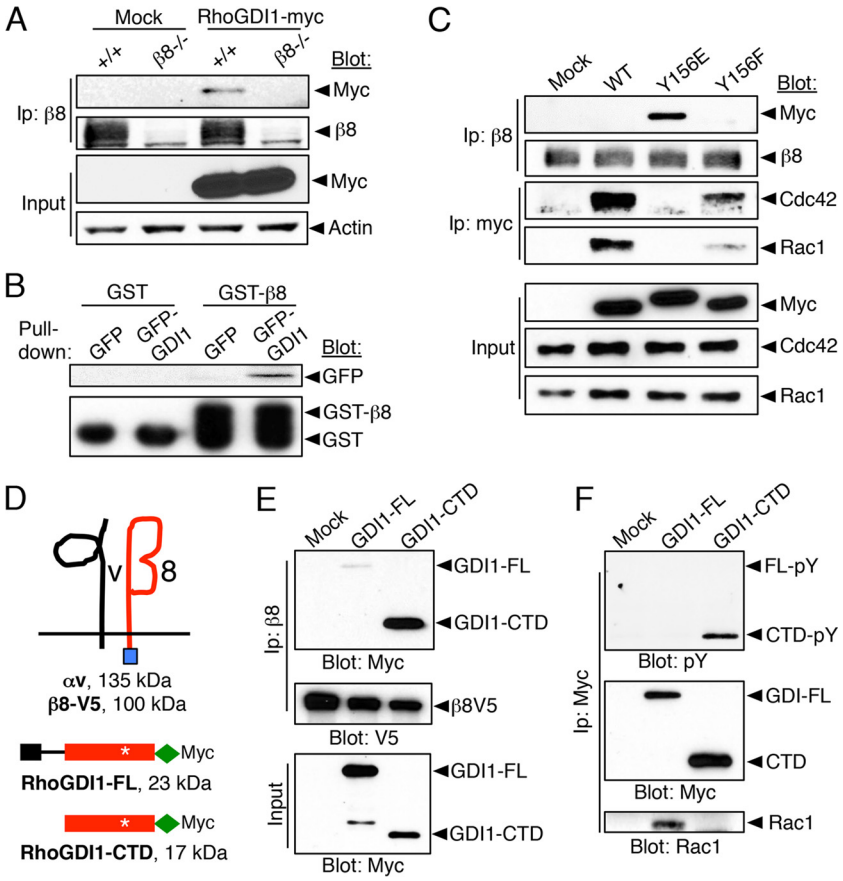

FIG 3 β8 integrin binds preferentially to RhoGDI1pY156 to regulate Rac1 and Cdc42 activation at the leading edge. (A, B) Myc-tagged RhoGDI1 protein binds to β8 integrin in wild-type astrocytes but not $\beta8^{-/-}$ cells, as revealed by coimmunoprecipitation (A) or pulldown assays using a recombinant protein consisting of GST fused to the cytoplasmic domain of β8 integrin (B). (C) Astrocytes were transfected with myc-tagged RhoGDI1 or Y156 point mutant constructs, and interactions with β8 integrin were analyzed by coimmunoprecipitation. Note that the mutant with the Y156E mutation showed enhanced binding to β8 integrin. A darker exposure would reveal relatively weak interactions with wild-type (WT) RhoGDI1. (D) Schematic showing constructs comprised of V5-tagged β8 integrin (100 kDa), myc-tagged full-length RhoGDI1 (21 kDa), or the 13-kDa myc-tagged RhoGDI1 CTD, which contains Y156 (asterisks). (E) V5-tagged β8 integrin interacts with full-length RhoGDI1 or the RhoGDI1 CTD, as revealed by coimmunoprecipitation. (F) In comparison to full-length RhoGDI1, the CTD of RhoGDI1 is hyperphosphorylated on tyrosine and binds weakly to Rac1. FL, Flag tag.

tained directional migration leading to a significant delay in wound closure (Fig. 1E and F).

αvβ8 integrin dampens Rac1 and Cdc42 activation at the leading edge. The cytoplasmic domain of β8 integrin is divergent from that of other integrins (see Fig. S1B in the supplemental material), suggesting signaling functions that are distinct from those of other integrins. Members of the Rho family of small GTPases regulate directional migration; therefore, we tested the hypothesis that migration defects in β8 integrin-deficient cells are linked to Rho GTPase signaling. Förster fluorescent resonance energy transfer (FRET) biosensors were used to quantify spatiotemporal patterns of integrin-dependent Cdc42 and Rac1 activation. Raichu-Cdc42 and Raichu-Rac1 consist of truncated Rho GTPase sequences fused to the Cdc42- and Rac-interactive binding domain (CRIB) of Pak1 flanked by YFP at the N terminus and CFP at the C terminus (36). Intramolecular interactions between endogenous GTP-bound Cdc42 and Rac1 and the CRIB domain juxtapose YFP and CFP, leading to FRET from CFP to YFP. In wild-type cells we detected spatially restricted patterns of active Cdc42 and Rac1 predominantly at membrane ruffles; in contrast, active Cdc42 and Rac1 distributed throughout the cell membrane, resulting in elevated total FRET in $\beta8^{-/-}$ cells (Fig. 2A; see also Movies S1 and S2 in the supplemental material). Raichu FRET biosensors are constitutively targeted to the membrane, and their activation state reflects the local balance between GEFs and GAPs; however, these probes are insensitive to RhoGDIs. Therefore, we visualized endogenous Cdc42 and Rac1 activation by TIRF microscopy in astrocytes expressing wGBD-enhanced GFP (EGFP) (40) and pYpet-PBD (41), respectively. These probes consist of the Cdc42-binding domain of WASP fused to EGFP (wGBD-EGFP) and the Rac-binding domain of Pak fused to the YFP variant (pYpet-PBD). As shown in Fig. 2B and Movies S3 and S4 in the supplemental material, activation of Cdc42 and Rac1 was significantly increased in $\beta8^{-/-}$ cells. Furthermore, the elevated Rac1 and Cdc42 signaling in $\beta8^{-/-}$ cells occurred primarily at the membrane (see Fig. S2 in the supplemental material).

αvβ8 integrin binds to RhoGDI1 with phosphorylated Y156 (RhoGDI1pY156). Our data that revealed that β8 integrin dampens Cdc42 and Rac1 signaling suggested a mechanism involving RhoGDI suppressive functions. Indeed, we detected interactions between β8 integrin and RhoGDI1 by immunoprecipitation and GST pulldown assays (Fig. 3A and B). RhoGDI1 protein pools that

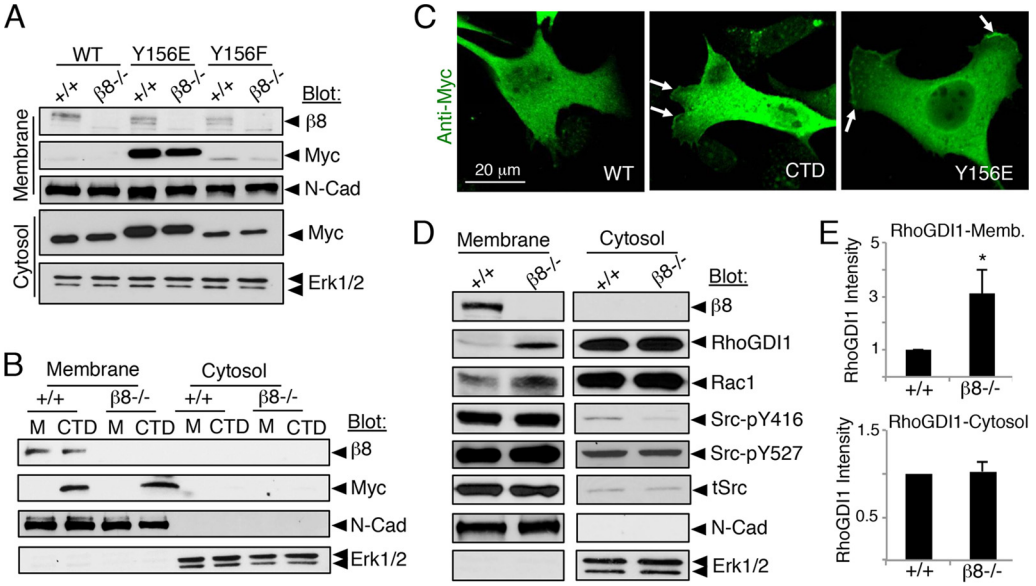

FIG 4 β8 integrin is dispensable for RhoGDI1 membrane recruitment but is essential for RhoGDI1 membrane release. (A) Membrane fractions from wild-type and $\beta8^{-/-}$ astrocytes expressing myc-tagged wild-type RhoGDI1 or Y156E or Y156F point mutants reveal that RhoGDI1Y156E localizes to membranes in an integrin-independent manner. (B) Cells were mock transfected (M) or transfected with plasmids expressing the CTD of RhoGDI1. Note the integrin-independent enrichment of the CTD at the plasma membrane. (C) Immunofluorescence staining of astrocytes expressing myc-tagged wild-type RhoGDI1 (left), the RhoGDI1 CTD truncation (center), or the RhoGDI1Y156E point mutation (right). Note that the Y156E and CTD mutant proteins are enriched at the cell membrane (arrows). (D) Membrane and cytosol fractions from wild-type or $\beta8^{-/-}$ astrocytes were immunoblotted for various signaling proteins, revealing elevated levels of RhoGDI1 and Rac1 proteins in $\beta8^{-/-}$ membranes. Integrin-dependent differences in total Src (tSrc) or phosphorylated Src variants were not detected. In these experiments, N-cadherin and Erk1/2 are controls showing exclusive expression in the membrane and cytosol, respectively. Membrane and cytosol fractions were analyzed in at least three different experiments. (E) Quantitation of RhoGDI1 protein levels in membrane (Memb.) and cytosol fractions from wild-type or $\beta8^{-/-}$ astrocytes (data are for immunoblots from three different lysates). Note that RhoGDI1 protein levels are elevated in $\beta8^{-/-}$ membrane fractions but not in cytosolic fractions. Error bars indicate SDs. *, $P < 0.05$.

are not complexed with Rho GTPases can be phosphorylated by Src on Y156, leading to RhoGDI1 recruitment to the leading edge (31). Interactions between β8 integrin and RhoGDI1 were tested with the phosphomimetic mutant, the RhoGDI1 protein with a Y156E mutation (RhoGDI1Y156E). In comparison to myc-tagged wild-type RhoGDI1 protein or the RhoGDI1 protein with a Y156F mutation (RhoGDI1Y156F), enhanced binding between β8 integrin and RhoGDI1Y156E was detected (Fig. 3C). The RhoGDI1Y156E variant also showed reduced binding to Rac1 and Cdc42 (Fig. 3C). RhoGDIs are comprised of N-terminal and C-terminal domains that control Rho extraction from the membrane and sequestration in the cytoplasm. Structural studies reveal that RhoGDIs are targeted to the membrane via their CTD, whereas the N-terminal domain mediates Rho extraction from the membrane and sequestration in the cytoplasm (46). To determine which domains of RhoGDI1 bind to the β8 integrin cytoplasmic tail, myc-tagged RhoGDI1 deletion mutants were generated (Fig. 3D). The N-terminal portion of RhoGDI1 containing amino acids 1 to 65 was not expressed in cells (data not shown), consistent with a prior report showing that this isolated region is susceptible to protease-mediated degradation (46). In contrast, the isolated CTD of RhoGDI1, which contains Y156, showed enhanced binding to β8 integrin (Fig. 3E). In comparison to full-length RhoGDI1, the isolated CTD was heavily tyrosine phosphorylated and showed reduced binding to Rac1 (Fig. 3F) and Cdc42 (data not shown).

αvβ8 integrin promotes RhoGDI1pY156 release from the membrane. To test whether αvβ8 integrin is necessary for recruitment of phosphorylated RhoGDI1 to the membrane, RhoGDI1 subcellular localization was quantified in wild-type and $\beta8^{-/-}$ cells. RhoGDI1 proteins (Y156E and CTD) were present in similar quantities in membrane fractions from wild-type and $\beta8^{-/-}$ cells, revealing that αvβ8 integrin is not essential for recruitment of tyrosine-phosphorylated RhoGDI1 (Fig. 4A and B). RhoGDI1Y156E and CTD protein variants were enriched at the astrocyte membrane, as revealed by immunofluorescence (Fig. 4C). Next, integrin-dependent levels of endogenous RhoGDI1 and other signaling effectors were analyzed in cytosolic and membrane fractions using phospho-specific antibodies (Fig. 4D). In comparison to control cells, elevated levels of RhoGDI1 and Rac1 proteins were detected in $\beta8^{-/-}$ membrane fractions but not in cytoplasmic fractions (Fig. 4D) or whole-cell lysates (data not shown). Densitometry revealed that the RhoGDI1 protein showed 3-fold enrichment in membranes fractionated from $\beta8^{-/-}$ cells (Fig. 4E). Integrin-dependent levels of active Src (phosphorylated Y416 [pY416]) or inactive Src (phosphorylated Y527 [pY527]) were not detected in membrane fractions. Collectively, these results show that αvβ8 integrin is not essential for recruitment of tyrosine-phosphorylated RhoGDI1 to the membrane but is necessary for the membrane release of RhoGDI1, likely via dynamic control of dephosphorylation via phosphatase activities.

β8 integrin forms a complex with PTP-PEST to regulate RhoGDI1 dephosphorylation. PTP-$PEST^{-/-}$ fibroblasts (MEFs) display hyperactive levels of Rac1, leading to impaired motility (6, 7). Therefore, we analyzed the roles for PTP-PEST in αvβ8 integrin-mediated regulation of RhoGDI1 functions. Protein interac-

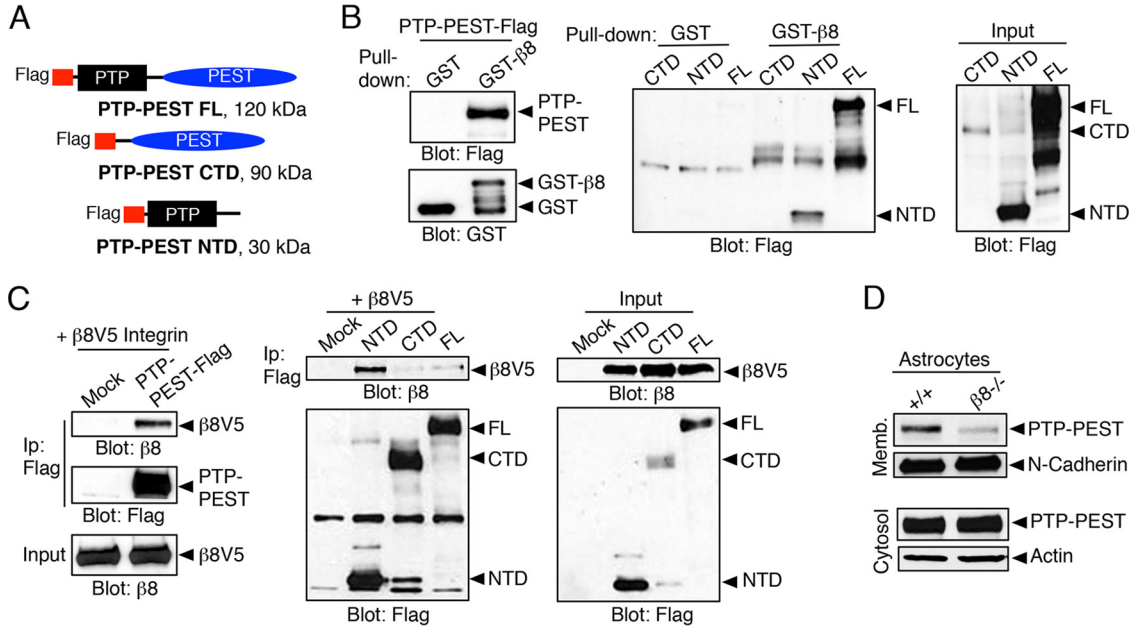

FIG 5 The β8 integrin cytoplasmic tail interacts with the PTP-PEST N-terminal domain. (A) Schematic diagram showing Flag-tagged full-length 120-kDa PTP-PEST (PTP-PEST FL) or truncated variants containing the 90-kDa CTD or the 30-kDa NTD. (B) Cell lysates containing Flag-tagged PTP-PEST were incubated with GST or GST-β8cyto. (Left) Anti-Flag immunoblotting reveals interactions between β8 integrin and PTP-PEST. (Middle and right) GST or GST-β8cyto proteins were tested for interactions with Flag-tagged PTP-PEST (FL) or the CTD and NTD mutants. Note that GST-β8cyto shows preferential binding with the isolated NTD. (C) (Left) Flag-tagged PTP-PEST and V5-tagged β8 integrin (β8V5) coimmunoprecipitate from transfected cell lysates. (Middle and right) Cotransfection analysis reveals that V5-tagged β8 integrin binds preferentially to the isolated NTD. (D) Endogenous PTP-PEST protein levels were analyzed in membrane and cytosol fractions from wild-type or $\beta8^{-/-}$ astrocytes. Note that PTP-PEST membrane localization is integrin dependent. All immunoprecipitation and GST pulldown experiments were performed at least three different times.

tions with αvβ8 integrin were tested using full-length PTP-PEST or deletion constructs consisting of the isolated N terminus containing the enzymatic domain (NTD) or the PEST-rich CTD (Fig. 5A). Full-length PTP-PEST and the isolated NTD bound to the β8 integrin cytoplasmic tail (Fig. 5B). Coimmunoprecipitation experiments also showed interactions between the NTD and V5-tagged β8 integrin. Interestingly, in comparison to full-length PTP-PEST, the isolated NTD showed enhanced binding to β8 integrin (Fig. 5C), suggesting that the PTP-PEST CTD may negatively regulate NTD interactions with β8 integrin. To determine if β8 integrin is necessary for recruiting PTP-PEST to the membrane, we fractionated the membranes and cytosol from control and $\beta8^{-/-}$ astrocytes. Membrane fractions from $\beta8^{-/-}$ cells contained significantly lower levels of PTP-PEST protein (Fig. 5D).

We next performed substrate-trapping experiments using wild-type or catalytically inactive PTP-PEST constructs. As shown in Fig. 6A, the GST-tagged D199A PTP-PEST variant but not wild-type PTP-PEST or the C231S variant interacted with the hyperphosphorylated RhoGDI1 CTD. Prior studies have shown that the D199A mutant shows higher affinities for phosphorylated substrates (47), which may account for its preferential binding to RhoGDI1 CTD. To further link PTP-PEST enzymatic activities to the RhoGDI1 phosphorylation cycle, we used recombinant GST-RhoGDI1 protein that was phosphorylated with purified Src and performed *in vitro* phosphatase assays using the catalytic domain of PTP-PEST. As shown in Fig. 6B, PTP-PEST catalyzed the tyrosine dephosphorylation of RhoGDI1. PTP-PEST protein is expressed at the leading edge of migrating astrocytes (Fig. 6C), and silencing its gene expression in astrocytes resulted in increased Rac1/Cdc42 signaling, as revealed by Pak hyperphosphorylation on serines 198 and 203 (Fig. 6D). Next, signaling in heterozygous control and PTP-$PEST^{-/-}$ MEFs was analyzed using an antibody recognizing phosphorylated Pak1. PTP-$PEST^{-/-}$ cells contained elevated levels of phosphorylated Pak protein (Fig. 6E) and showed defective cell migration in scratch-wound assays (see Fig. S3 in the supplemental material), findings consistent with previous reports (6, 48). Analysis of cells expressing constitutively activate Src (Y527F mutant cells) revealed elevated levels of tyrosine-phosphorylated RhoGDI1 protein in PTP-PEST-null MEFs (Fig. 6F). Forced expression of Flag-tagged PTP-PEST in null MEFs resulted in diminished levels of tyrosine-phosphorylated RhoGDI1 (Fig. 6G).

Links between β8 integrin, PTP-PEST, and RhoGDI1 phosphorylation were also analyzed in explants taken from the mouse brain SVZ. Astrocyte-like progenitor cells in the SVZ give rise to neuroblasts that migrate directionally to the olfactory bulbs via the RMS (49), and SVZ tissue explants show robust migration *ex vivo* (see Fig. S4 in the supplemental material). Neuroblasts sorted from the SVZ express β8 integrin, and integrin protein was detected mainly at the leading edge of migrating cells (see Fig. S8 in the supplemental material). SVZ explants were dissected from wild-type and $\beta8^{-/-}$ mice, and integrin-dependent cell migration was quantified. In comparison to control SVZ explants, $\beta8^{-/-}$ explants showed obvious defects in sustained migration (Fig. 7A; see also Fig. S4 in the supplemental material). SVZ regions isolated from nestin-Cre; $\alpha v^{flox/flox}$ and nestin-Cre; $\beta8^{flox/flox}$ conditional mutant mice also displayed obvious migration defects (see Fig. S5 in the supplemental material). To further link cell migration de-

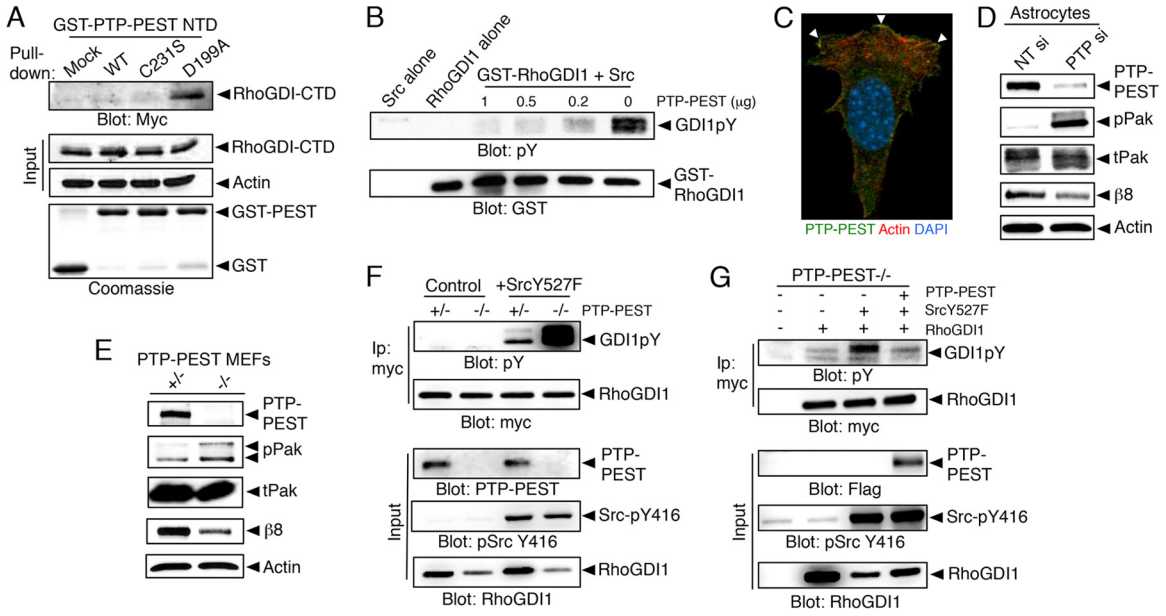

FIG 6 Integrin-bound PTP-PEST dephosphorylates RhoGDI1. (A) Substrate trapping experiments with the wild-type PTP-PEST catalytic domain or catalytically inactive point mutants reveal binding between the hyperphosphorylated RhoGDI1 CTD and the D199A mutant construct. (B) The PTP-PEST catalytic domain promotes dephosphorylation of the Src-phosphorylated RhoGDI1 protein *in vitro*. The GST-RhoGDI1 protein was tyrosine phosphorylated *in vitro* by mixing with purified Src and ATP. GST-RhoGDI1 complexes were then incubated with various amounts of the PTP-PEST catalytic domain. Glutathione-agarose was used to fractionate GST-RhoGDI1, and proteins were immunoblotted with anti-GST or anti-pY antibodies. Controls were Src alone or GST-RhoGDI1 alone in the absence of PTP-PEST. (C) Mouse astrocytes transfected with a Flag-tagged PTP-PEST construct show PTP-PEST protein enrichment at the membrane. DAPI, 4′,6-diamidino-2-phenylindole. (D) Silencing of PTP-PEST gene expression in astrocytes using siRNAs leads to increased levels of phosphorylated Pak, indicating hyperactive Rac1/Cdc42 signaling. Also note the decrease in β8 integrin protein levels after PTP-PEST silencing. All immunoprecipitation and GST pulldown experiments were performed at least three different times. Nontargeting (NT) si and PTP si, siRNAs specific for NT and PTP. (E) MEFs genetically null for PTP-PEST show elevated levels of pPak proteins and express reduced levels of β8 integrin protein. (F) The levels of tyrosine-phosphorylated RhoGDI1 in control or PTP-PEST$^{-/-}$ MEFs expressing RhoGDI1-myc and constitutively active Src (Y527F mutant cells) were analyzed. Note that cells lacking PTP-PEST show elevated levels of tyrosine-phosphorylated RhoGDI1. (G) PTP-PEST$^{-/-}$ MEFs stably expressing constitutively active Src (Y527F mutant cells) show elevated levels of tyrosine-phosphorylated RhoGDI1 protein. These levels are reduced upon forced expression of PTP-PEST.

fects to the RhoGDI1 phosphorylation cycle, SVZ explants were treated with dasatinib, a small-molecule kinase inhibitor that shows specificity for Src family kinases (50). Dasatinib significantly blocked cell migration from SVZ explants (Fig. 7B), and this correlated with reduced levels of tyrosine-phosphorylated Src and RhoGDI1 (Fig. 7C; see also Fig. S6 in the supplemental material). SVZ explants were also treated with a synthetic molecule that blocks the enzymatic activities of PTP-PEST (51). Pharmacologic inhibition of PTP-PEST resulted in the blockade of cell migration from SVZ explants (see Fig. S6 in the supplemental material). We attempted to rescue β8 integrin-dependent neuroblast migration defects using NSC23766, a synthetic inhibitor of the Rac1 GEF Tiam1. However, treatment of β8$^{-/-}$ SVZ explants with NSC23766 did not restore cell migration (see Fig. S7 in the supplemental material), highlighting that a precise balance of Rac1 and Cdc42 activation is necessary for control of motility.

Given the importance of β8 integrin control of TGFβ activation and signaling in brain vascular development (52), we next analyzed roles for TGFβ signaling in neural cell migration using an anti-TGFβ neutralizing antibody that blocks canonical TGFβ receptor signaling (Fig. 7D). However, inhibition of TGFβ signaling did not inhibit cell migration from the SVZ in *ex vivo* assays (Fig. 7E). Conditional ablation of the Tgfbr2$^{flox/flox}$ gene in neural cells via nestin-Cre did not impact neuroblast migration from the SVZ to the olfactory bulbs (see Fig. S9 in the supplemental material). Furthermore, inducible deletion ablation of Tgfbr2 in endothelial cells, which results in brain vascular pathologies (15), did not cause neuroblast migration defects in the RMS (H. S. Lee and J. H. McCarty, unpublished data). Collectively, these data support our model in which the RhoGDI1 phosphorylation cycle regulated by Src and the αvβ8 integrin-PTP-PEST complex is essential for control of cell migration but indicate that these events occur via TGFβ-independent adhesion and signaling.

β8 integrin is essential for directional cell migration *in vivo*. Next, β8 integrin control of directional cell migration was analyzed *in vivo*. Neuroblast migration defects were apparent in the β8$^{-/-}$ RMS, as revealed by anti-Dcx immunofluorescence (Fig. 8A and B). β8$^{-/-}$ cells failed to form well-organized chains and often dispersed as individual cells, resulting in a disorganized RMS cytoarchitecture (Fig. 8C), with fewer Dcx-positive cells being found in the olfactory bulbs (Fig. 8D). Prior reports have shown that blood vessels guide migrating neuroblasts (53, 54); however, cell migration defects in β8$^{-/-}$ mice were not due to obvious blood vessel patterning defects (see Fig. S8A and B in the supplemental material). A nestin-Cre transgene (42), which is active in RMS neuroblasts (see Fig. S8D in the supplemental material), was used to conditionally ablate β8$^{flox/flox}$ and αv$^{flox/flox}$ genes. Nestin-Cre; β8$^{flox/flox}$ and nestin-Cre; αv$^{flox/flox}$ conditional knockouts developed cell migration defects in the RMS similar to whole-body β8$^{-/-}$ mice (see Fig. S5 in the supplemental material). Immunoblotting of SVZ/RMS lysates prepared from β8$^{-/-}$ mice (n = 4 per genotype) revealed increased Pak phosphorylation

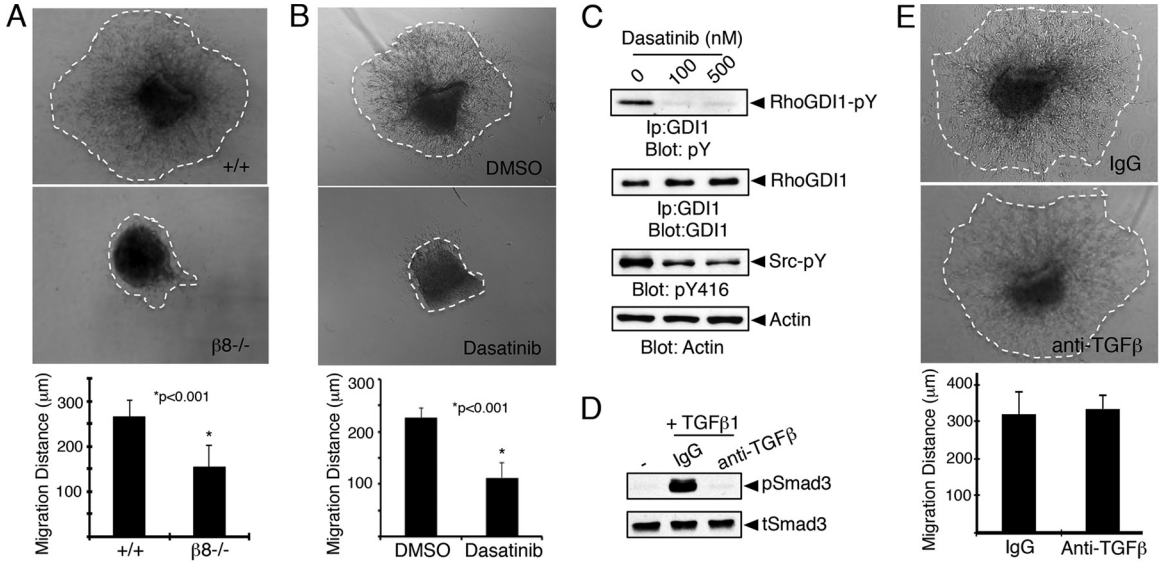

FIG 7 Inhibition of β8 integrin gene expression or RhoGDI1 tyrosine phosphorylation blocks cell migration in tissue explants. (A) SVZ explants from wild-type or $\beta8^{-/-}$ mice were assayed for migration in a three-dimensional Matrigel. Note that $\beta8^{-/-}$ explants show statistically significant defects in neural cell migration. (B) Brain SVZ explants from wild-type mice were assayed for migration in a three-dimensional Matrigel with dasatinib (1 μM). Src family kinase inhibition results in statistically significant cell migration defects. DMSO, dimethyl sulfoxide. *, $P < 0.01$. (C) Astrocytes were treated with various doses of dasatinib and the phosphatase inhibitor pervanadate. Levels of Src autophosphorylation (pY416) and RhoGDI1pY were then analyzed by immunoblotting. (D) Neurospheres were cultured from the SVZ and treated with TGFβ1 (2 ng/ml) in the presence of control IgGs and anti-TGFβ antibodies. Note that TGFβ neutralization blocks Smad activation, as determined by anti-phospho-Smad3 immunoblotting. tSmad3, total pSmad3; pSmad3, phosphorylated Smad3. (E) SVZ explants were embedded in Matrigel in the presence of 10 μg/ml control IgG (top) or anti-TGFβ neutralizing antibody (bottom). There were no statistically significant differences in cell migration following TGFβ inhibition.

(Fig. 8E and F), indicating hyperactive Rac1/Cdc42 signaling. Immunofluorescence staining of fixed brain sections revealed RhoGDI1 protein expression in neuroblasts in the RMS (Fig. 8G). Collectively, these *in vivo* and *in vitro* data reveal that regulation of the RhoGDI1 phosphorylation cycle is essential for control of directional cell motility (Fig. 8H).

DISCUSSION

Here, we have characterized an adhesion and signaling unit comprised of PTP-PEST, β8 integrin, and RhoGDI1 that controls the spatiotemporal patterns of Rac1/Cdc42 activation in directionally migrating cells. Our experiments reveal the following novel findings: (i) αvβ8 integrin localizes to the cell leading edge and is essential for directional motility *in vitro* (Fig. 1); (ii) FRET imaging reveals that β8 integrin dampens Rac1 and Cdc42 activation at the leading edge, with $\beta8^{-/-}$ cells displaying elevated levels and mislocalized patterns of GTP-bound Rac1 and Cdc42 (Fig. 2); (iii) β8 integrin binds with a high affinity to the CTD of RhoGDI1 that is phosphorylated on Y156 by Src (Fig. 3 and 4); (iv) interactions with β8 integrin at the cell leading edge promote RhoGDI1 dephosphorylation via integrin-bound PTP-PEST, resulting in RhoGDI1 release from the membrane (Fig. 5 and 6); (v) perturbing the RhoGDI1 phosphorylation cycle by genetic ablation of β8 integrin or pharmacologic inhibition of PTP-PEST or Src leads to cell migration defects *ex vivo* (Fig. 7; see also Fig. S6 in the supplemental material); and (vi) mice genetically null for β8 integrin display neuroblast migration defects *in vivo* due, in part, to hyperactivation of Rac1 and Cdc42 (Fig. 8). Collectively, these data identify the αvβ8 integrin-PTP-PEST protein complex to be a regulatory switch that spatiotemporally controls RhoGDI functions at the leading edge.

A prior study has shown that RGD-containing peptides inhibit astrocyte polarity and directional migration, although the exact integrin heterodimers and ECM protein ligands involved in these events were not identified (55). While β8 integrin is essential for directional migration, we have not found β8 integrin-dependent defects in astrocyte polarity (data not shown), revealing that adhesion/signaling pathways controlled by other RGD-binding integrins are involved in cell polarization. Interestingly, we have found that astrocytes lacking all αv-containing integrins display a complete failure to polarize and migrate (data not shown). αϖβ3 integrin activates Rac1 by facilitating interactions with GEFs at the leading edge, with RhoGDIs suppressing Rac1 membrane localization (56, 57). On the basis of these data, it is enticing to speculate that the αvβ8 integrin-PTP-PEST complex cross talks with the αvβ3 integrin pathway to cooperatively regulate subcellular localization of RhoGDI and facilitate spatiotemporal Rac1 interactions with GEFs.

Given the importance of integrin activation of latent TGFβs in brain development (58), we assumed that integrin control of cell migration would be dependent on TGFβ signaling. However, our *in vitro* and *in vivo* data revealed apparently normal cell migration following TGFβ blockade and TGFβ receptor gene deletion (Fig. 7; see also Fig. S9 in the supplemental material). Therefore, ECM protein ligands other than latent TGFβs are involved in integrin signaling via PTP-PEST, RhoGDIs, and probably other effectors. Interestingly, the extracellular region of β8 integrin lacks a deadbolt domain that in other integrins suppresses adhesion until signaling proteins induce inside-out structural changes that activate ECM adhesion (59). Hence, αvβ8 integrin may be constitutively active and signal via PTP-PEST, RhoGDI1, and other effectors possibly via ECM-independent mechanisms.

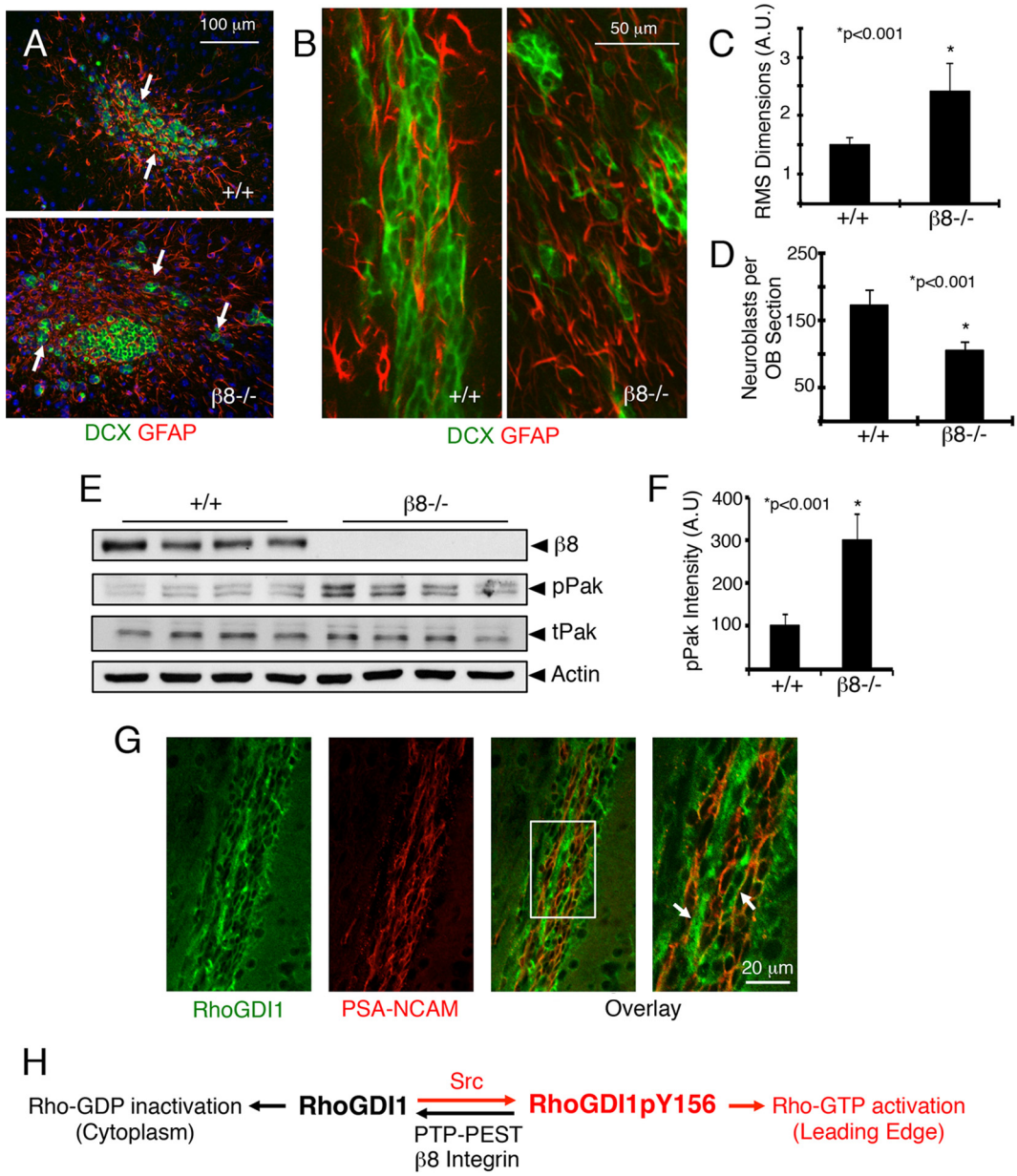

FIG 8 β8 integrin promotes directional cell migration *in vivo*. (A) Representative coronal sections through the RMS of wild-type and $\beta8^{-/-}$ mice stained with anti-Dcx and anti-glial fibrillary acidic protein (anti-GFAP) reveal neuroblasts and astrocytes, respectively, in the RMS. Note the neural cell migration defects in $\beta8^{-/-}$ mice. (B) Representative sagittal sections through the RMS of wild-type and $\beta8^{-/-}$ mice labeled with anti-Dcx and anti-GFAP antibodies. Note the abnormal clusters of neuroblasts in $\beta8^{-/-}$ brain sections. (C, D) Quantitation of integrin-dependent neuroblast migration defects in the RMS (C) and olfactory bulbs (OBs) (D). (E) Tissue lysates were prepared from the SVZ/RMS of wild-type and $\beta8^{-/-}$ mice and immunoblotted with anti-phospho-Pak, a readout for Rac1/Cdc42 activation. tPak, total Pak; pPak, phosphorylated Pak. (F) Quantitation of integrin-dependent phospho-Pak protein levels. (G) RhoGDI1 protein is expressed in neuroblasts in the mouse rostral migratory stream, as revealed by colocalization with polysialylated neural cell adhesion molecule (PSA-NCAM). The right image is a higher-magnification image of the white boxed area. Arrows indicate neuroblasts expressing RhoGDI1 and PSA-NCAM. (H) In migrating cells, Src phosphorylation of RhoGDI1 on Y156 leads to deposition of Rac1/Cdc42 proteins at the leading edge, enabling their activation. RhoGDI1pY156 also translocates to the leading edge, where it is coupled to PTP-PEST via interactions with αvβ8 integrin, which facilitates RhoGDI1 dephosphorylation, release from the membrane, and subsequent suppression of Rac1/Cdc42 signaling in the cytoplasm. Collectively, these events control the spatiotemporal patterns of Rac1/Cdc42 activation to promote directional cell motility.

Growth factors, including epidermal growth factor (EGF) and platelet-derived growth factor, activate Src to promote tyrosine phosphorylation of RhoGDI1 (31). β8 integrin is dispensable for Src-mediated RhoGDI1 phosphorylation, and we have not detected protein complexes between β8 integrin and Src (data not shown). We propose that the αvβ8 integrin-PTP-PEST protein complex is a hub for modulating signaling by Rac1/Cdc42 and other promigratory effectors at the leading edge. RhoGDI1 is a key intracellular substrate for PTP-PEST; however, additional proteins and possibly other Rho effectors are likely dephosphorylated

by integrin-bound PTP-PEST to promote motility. For example, PTP-PEST dephosphorylates and inactivates the Rho GEF Vav2 and the Rho GAP p190 (7) as well as the p120 catenin, which may have RhoGDI-like functions (10). Interestingly, in astrocytes and MEFs that express diminished levels of PTP-PEST (Fig. 6), we detected decreased β8 integrin protein, suggesting that PTP-PEST may regulate integrin protein stability and/or gene expression. PTP-PEST is reported to dephosphorylate epidermal growth factor receptor (EGFR) to suppress kinase activities (60). Hence, it is possible that integrin-bound PTP-PEST is a component of a signaling loop that dampens EGFR-induced Src activities. EGFR suppresses neuroblast migration in the SVZ (61), but how this suppression is relieved in migrating cells remains unknown. Interestingly, $\beta8^{-/-}$ neuroblasts cluster in the SVZ, and neurospheres cultured from $\beta8^{-/-}$ mice fail to proliferate/self-renew in EGF-containing media (18). Hence, integrin-bound PTP-PEST may dephosphorylate EGFR to regulate its tyrosine kinase activities and control cell growth in the SVZ and migration in the RMS.

Lastly, while our experiments have focused on components of the αvβ8 integrin-PTP-PEST signaling complex in neural cells, this pathway likely drives migration in other nonneural cell types. RhoGDIs and PTP-PEST are broadly expressed, and αvβ8 integrin plays important roles in tissue development and pathophysiology outside the nervous system. For example, dendritic cells utilize αvβ8 integrin to traffic through the intestine and colon to control normal homeostasis, with ablation of αv or β8 integrin gene expression in immune cells leading to autoimmunity and cancer (62, 63). While these pathologies have largely been attributed to defective latent TGFβ activation (64), αvβ8 integrin-dependent intracellular signaling pathways may also play roles in immune cell migration during homeostatic surveillance. A recent report has shown that deletion of PTP-PEST in dendritic cells leads to defective migration and spontaneous autoimmunity in mice (65). In addition, αvβ8 integrin signals via the effector protein Band 4.1B during embryonic heart morphogenesis (66), likely in migratory cardiac neural crest cells. Primary tumors in the lung, mouth, skin, and other organs commonly upregulate β8 integrin gene expression during metastatic dispersal, and inhibition of integrin expression diminishes metastasis (67–70). Hence, the αvβ8 integrin-PTP-PEST-RhoGDI1 signaling unit probably modulates leading edge dynamics and motility in divergent cell types.

ACKNOWLEDGMENTS

We thank Gary Gallick for providing dasatinib, Martin Schwartz for providing the GFP-RhoGDI1 construct, Sarita Sastry for providing the PTP-PEST substrate-trapping constructs (wild type and C231S), and Kim Tolias for providing the phospho-Pak antibody.

This research was supported by grants awarded to J.H.M. from the National Institute of Neurological Disorders and Stroke (R01NS059876 and R01NS078402), the National Cancer Institute (P50CA127001), and The Cancer Prevention and Research Institute of Texas (RP140411), to C.D. from the National Institute of General Medicine (R01GM099837), and to G.M.R. (AHA0325791T) from the American Heart Association.

REFERENCES

1. **Ostman A, Hellberg C, Bohmer FD.** 2006. Protein-tyrosine phosphatases and cancer. Nat Rev Cancer **6:**307–320. http://dx.doi.org/10.1038/nrc1837.
2. **Tonks NK.** 2006. Protein tyrosine phosphatases: from genes, to function, to disease. Nat Rev Mol Cell Biol **7:**833–846. http://dx.doi.org/10.1038/nrm2039.
3. **Zheng Y, Lu Z.** 2013. Regulation of tumor cell migration by protein tyrosine phosphatase (PTP)-proline-, glutamate-, serine-, and threonine-rich sequence (PEST). Chin J Cancer **32:**75–83. http://dx.doi.org/10.5732/cjc.012.10084.
4. **Sirois J, Cote JF, Charest A, Uetani N, Bourdeau A, Duncan SA, Daniels E, Tremblay ML.** 2006. Essential function of PTP-PEST during mouse embryonic vascularization, mesenchyme formation, neurogenesis and early liver development. Mech Dev **123:**869–880. http://dx.doi.org/10.1016/j.mod.2006.08.011.
5. **Souza CM, Davidson D, Rhee I, Gratton JP, Davis EC, Veillette A.** 2012. The phosphatase PTP-PEST/PTPN12 regulates endothelial cell migration and adhesion, but not permeability, and controls vascular development and embryonic viability. J Biol Chem **287:**43180–43190. http://dx.doi.org/10.1074/jbc.M112.387456.
6. **Sastry SK, Lyons PD, Schaller MD, Burridge K.** 2002. PTP-PEST controls motility through regulation of Rac1. J Cell Sci **115:**4305–4316. http://dx.doi.org/10.1242/jcs.00105.
7. **Sastry SK, Rajfur Z, Liu BP, Cote JF, Tremblay ML, Burridge K.** 2006. PTP-PEST couples membrane protrusion and tail retraction via VAV2 and p190RhoGAP. J Biol Chem **281:**11627–11636. http://dx.doi.org/10.1074/jbc.M600897200.
8. **Jamieson JS, Tumbarello DA, Halle M, Brown MC, Tremblay ML, Turner CE.** 2005. Paxillin is essential for PTP-PEST-dependent regulation of cell spreading and motility: a role for paxillin kinase linker. J Cell Sci **118:**5835–5847. http://dx.doi.org/10.1242/jcs.02693.
9. **Zheng Y, Xia Y, Hawke D, Halle M, Tremblay ML, Gao X, Zhou XZ, Aldape K, Cobb MH, Xie K, He J, Lu Z.** 2009. FAK phosphorylation by ERK primes ras-induced tyrosine dephosphorylation of FAK mediated by PIN1 and PTP-PEST. Mol Cell **35:**11–25. http://dx.doi.org/10.1016/j.molcel.2009.06.013.
10. **Espejo R, Jeng Y, Paulucci-Holthauzen A, Rengifo-Cam W, Honkus K, Anastasiadis PZ, Sastry SK.** 2013. PTP-PEST targets a novel tyrosine site in p120 catenin to control epithelial cell motility and Rho GTPase activity. J Cell Sci **127**(Pt 3)**:**497–508. http://dx.doi.org/10.1242/jcs.120154.
11. **Hynes RO.** 2009. The extracellular matrix: not just pretty fibrils. Science **326:**1216–1219. http://dx.doi.org/10.1126/science.1176009.
12. **Moyle M, Napier MA, McLean JW.** 1991. Cloning and expression of a divergent integrin subunit beta 8. J Biol Chem **266:**19650–19658.
13. **Nishimura SL, Sheppard D, Pytela R.** 1994. Integrin alpha v beta 8. Interaction with vitronectin and functional divergence of the beta 8 cytoplasmic domain. J Biol Chem **269:**28708–28715.
14. **Worthington JJ, Klementowicz JE, Travis MA.** 2011. TGFbeta: a sleeping giant awoken by integrins. Trends Biochem Sci **36:**47–54. http://dx.doi.org/10.1016/j.tibs.2010.08.002.
15. **Allinson K, Lee H, Fruttiger M, McCarty J, Arthur H.** 2012. Endothelial expression of TGFβ type II receptor is required to maintain vascular integrity during postnatal development of the central nervous system. PLoS One **7:**e39336. http://dx.doi.org/10.1371/journal.pone.0039336.
16. **Arnold TD, Ferrero GM, Qiu H, Phan IT, Akhurst RJ, Huang EJ, Reichardt LF.** 2012. Defective retinal vascular endothelial cell development as a consequence of impaired integrin alphaVbeta8-mediated activation of transforming growth factor-beta. J Neurosci **32:**1197–1206. http://dx.doi.org/10.1523/JNEUROSCI.5648-11.2012.
17. **McCarty JH, Lacy-Hulbert A, Charest A, Bronson RT, Crowley D, Housman D, Savill J, Roes J, Hynes RO.** 2005. Selective ablation of alphav integrins in the central nervous system leads to cerebral hemorrhage, seizures, axonal degeneration and premature death. Development **132:**165–176. http://dx.doi.org/10.1242/dev.01551.
18. **Mobley AK, Tchaicha JH, Shin J, Hossain MG, McCarty JH.** 2009. Beta8 integrin regulates neurogenesis and neurovascular homeostasis in the adult brain. J Cell Sci **122:**1842–1851. http://dx.doi.org/10.1242/jcs.043257.
19. **Nguyen HL, Lee YJ, Shin J, Lee E, Park SO, McCarty JH, Oh SP.** 2011. TGF-beta signaling in endothelial cells, but not neuroepithelial cells, is essential for cerebral vascular development. Lab Invest **91:**1554–1563. http://dx.doi.org/10.1038/labinvest.2011.124.
20. **Proctor JM, Zang K, Wang D, Wang R, Reichardt LF.** 2005. Vascular development of the brain requires beta8 integrin expression in the neuroepithelium. J Neurosci **25:**9940–9948. http://dx.doi.org/10.1523/JNEUROSCI.3467-05.2005.
21. **Su H, Kim H, Pawlikowska L, Kitamura H, Shen F, Cambier S, Markovics J, Lawton MT, Sidney S, Bollen AW, Kwok PY, Reichardt L, Young WL, Yang GY, Nishimura SL.** 2010. Reduced expression of integrin alphavbeta8 is associated with brain arteriovenous malformation

pathogenesis. Am J Pathol **176:**1018–1027. http://dx.doi.org/10.2353/ajpath.2010.090453.
22. **Reyes SB, Narayanan AS, Lee HS, Tchaicha JH, Aldape KD, Lang FF, Tolias KF, McCarty JH.** 2013. Alphavbeta8 integrin interacts with RhoGDI1 to regulate Rac1 and Cdc42 activation and drive glioblastoma cell invasion. Mol Biol Cell **24:**474–482. http://dx.doi.org/10.1091/mbc.E12-07-0521.
23. **Tchaicha JH, Reyes SB, Shin J, Hossain MG, Lang FF, McCarty JH.** 2011. Glioblastoma angiogenesis and tumor cell invasiveness are differentially regulated by beta8 integrin. Cancer Res **71:**6371–6381. http://dx.doi.org/10.1158/0008-5472.CAN-11-0991.
24. **Upadhyaya M, Spurlock G, Thomas L, Thomas NS, Richards M, Mautner VF, Cooper DN, Guha A, Yan J.** 2012. Microarray-based copy number analysis of neurofibromatosis type-1 (NF1)-associated malignant peripheral nerve sheath tumors reveals a role for Rho-GTPase pathway genes in NF1 tumorigenesis. Hum Mutat **33:**763–776. http://dx.doi.org/10.1002/humu.22044.
25. **Harburger DS, Calderwood DA.** 2009. Integrin signalling at a glance. J Cell Sci **122:**159–163. http://dx.doi.org/10.1242/jcs.018093.
26. **Kim C, Ye F, Ginsberg MH.** 2011. Regulation of integrin activation. Annu Rev Cell Dev Biol **27:**321–345. http://dx.doi.org/10.1146/annurev-cellbio-100109-104104.
27. **Lakhe-Reddy S, Khan S, Konieczkowski M, Jarad G, Wu KL, Reichardt LF, Takai Y, Bruggeman LA, Wang B, Sedor JR, Schelling JR.** 2006. Beta8 integrin binds Rho GDP dissociation inhibitor-1 and activates Rac1 to inhibit mesangial cell myofibroblast differentiation. J Biol Chem **281:**19688–19699. http://dx.doi.org/10.1074/jbc.M601110200.
28. **DerMardirossian C, Bokoch GM.** 2005. GDIs: central regulatory molecules in Rho GTPase activation. Trends Cell Biol **15:**356–363. http://dx.doi.org/10.1016/j.tcb.2005.05.001.
29. **Boulter E, Garcia-Mata R, Guilluy C, Dubash A, Rossi G, Brennwald PJ, Burridge K.** 2010. Regulation of Rho GTPase crosstalk, degradation and activity by RhoGDI1. Nat Cell Biol **12:**477–483. http://dx.doi.org/10.1038/ncb2049.
30. **Garcia-Mata R, Boulter E, Burridge K.** 2011. The 'invisible hand': regulation of RHO GTPases by RHOGDIs. Nat Rev Mol Cell Biol **12:**493–504. http://dx.doi.org/10.1038/nrm3153.
31. **DerMardirossian C, Rocklin G, Seo JY, Bokoch GM.** 2006. Phosphorylation of RhoGDI by Src regulates Rho GTPase binding and cytosol-membrane cycling. Mol Biol Cell **17:**4760–4768. http://dx.doi.org/10.1091/mbc.E06-06-0533.
32. **McCarty JH, Cook AA, Hynes RO.** 2005. An interaction between {alpha}v{beta}8 integrin and Band 4.1B via a highly conserved region of the Band 4.1 C-terminal domain. Proc Natl Acad Sci U S A **102:**13479–13483. http://dx.doi.org/10.1073/pnas.0506068102.
33. **Tchaicha JH, Mobley AK, Hossain MG, Aldape KD, McCarty JH.** 2010. A mosaic mouse model of astrocytoma identifies alphavbeta8 integrin as a negative regulator of tumor angiogenesis. Oncogene **29:**4460–4472. http://dx.doi.org/10.1038/onc.2010.199.
34. **Shamah SM, Lin MZ, Goldberg JL, Estrach S, Sahin M, Hu L, Bazalakova M, Neve RL, Corfas G, Debant A, Greenberg ME.** 2001. EphA receptors regulate growth cone dynamics through the novel guanine nucleotide exchange factor ephexin. Cell **105:**233–244. http://dx.doi.org/10.1016/S0092-8674(01)00314-2.
35. **Mobley AK, McCarty JH.** 2011. Beta8 integrin is essential for neuroblast migration in the rostral migratory stream. Glia **59:**1579–1587. http://dx.doi.org/10.1002/glia.21199.
36. **Aoki K, Matsuda M.** 2009. Visualization of small GTPase activity with fluorescence resonance energy transfer-based biosensors. Nat Protoc **4:**1623–1631. http://dx.doi.org/10.1038/nprot.2009.175.
37. **Chaki SP, Barhoumi R, Berginski ME, Sreenivasappa H, Trache A, Gomez SM, Rivera GM.** 2013. Nck enables directional cell migration through the coordination of polarized membrane protrusion with adhesion dynamics. J Cell Sci **126:**1637–1649. http://dx.doi.org/10.1242/jcs.119610.
38. **Allen RJ, Tsygankov D, Zawistowski JS, Elston TC, Hahn KM.** 2014. Automated line scan analysis to quantify biosensor activity at the cell edge. Methods **66:**162–167. http://dx.doi.org/10.1016/j.ymeth.2013.08.025.
39. **Hodgson L, Pertz O, Hahn KM.** 2008. Design and optimization of genetically encoded fluorescent biosensors: GTPase biosensors. Methods Cell Biol **85:**63–81. http://dx.doi.org/10.1016/S0091-679X(08)85004-2.
40. **Benink HA, Bement WM.** 2005. Concentric zones of active RhoA and Cdc42 around single cell wounds. J Cell Biol **168:**429–439. http://dx.doi.org/10.1083/jcb.200411109.
41. **Machacek M, Hodgson L, Welch C, Elliott H, Pertz O, Nalbant P, Abell A, Johnson GL, Hahn KM, Danuser G.** 2009. Coordination of Rho GTPase activities during cell protrusion. Nature **461:**99–103. http://dx.doi.org/10.1038/nature08242.
42. **Tronche F, Kellendonk C, Kretz O, Gass P, Anlag K, Orban PC, Bock R, Klein R, Schutz G.** 1999. Disruption of the glucocorticoid receptor gene in the nervous system results in reduced anxiety. Nat Genet **23:**99–103. http://dx.doi.org/10.1038/12703.
43. **Chytil A, Magnuson MA, Wright CV, Moses HL.** 2002. Conditional inactivation of the TGF-beta type II receptor using Cre:Lox. Genesis **32:**73–75. http://dx.doi.org/10.1002/gene.10046.
44. **Gong S, Zheng C, Doughty ML, Losos K, Didkovsky N, Schambra UB, Nowak NJ, Joyner A, Leblanc G, Hatten ME, Heintz N.** 2003. A gene expression atlas of the central nervous system based on bacterial artificial chromosomes. Nature **425:**917–925. http://dx.doi.org/10.1038/nature02033.
45. **Liang CC, Park AY, Guan JL.** 2007. In vitro scratch assay: a convenient and inexpensive method for analysis of cell migration in vitro. Nat Protoc **2:**329–333. http://dx.doi.org/10.1038/nprot.2007.30.
46. **Gosser YQ, Nomanbhoy TK, Aghazadeh B, Manor D, Combs C, Cerione RA, Rosen MK.** 1997. C-terminal binding domain of Rho GDP-dissociation inhibitor directs N-terminal inhibitory peptide to GTPases. Nature **387:**814–819. http://dx.doi.org/10.1038/42961.
47. **Blanchetot C, Chagnon M, Dube N, Halle M, Tremblay ML.** 2005. Substrate-trapping techniques in the identification of cellular PTP targets. Methods **35:**44–53. http://dx.doi.org/10.1016/j.ymeth.2004.07.007.
48. **Zheng Y, Yang W, Xia Y, Hawke D, Liu DX, Lu Z.** 2011. Ras-induced and extracellular signal-regulated kinase 1 and 2 phosphorylation-dependent isomerization of protein tyrosine phosphatase (PTP)-PEST by PIN1 promotes FAK dephosphorylation by PTP-PEST. Mol Cell Biol **31:**4258–4269. http://dx.doi.org/10.1128/MCB.05547-11.
49. **Murase S, Horwitz AF.** 2004. Directions in cell migration along the rostral migratory stream: the pathway for migration in the brain. Curr Top Dev Biol **61:**135–152. http://dx.doi.org/10.1016/S0070-2153(04)61006-4.
50. **Buettner R, Mesa T, Vultur A, Lee F, Jove R.** 2008. Inhibition of Src family kinases with dasatinib blocks migration and invasion of human melanoma cells. Mol Cancer Res **6:**1766–1774. http://dx.doi.org/10.1158/1541-7786.MCR-08-0169.
51. **Karver MR, Krishnamurthy D, Kulkarni RA, Bottini N, Barrios AM.** 2009. Identifying potent, selective protein tyrosine phosphatase inhibitors from a library of Au(I) complexes. J Med Chem **52:**6912–6918. http://dx.doi.org/10.1021/jm901220m.
52. **McCarty JH.** 2009. Integrin-mediated regulation of neurovascular development, physiology and disease. Cell Adh Migr **3:**211–215. http://dx.doi.org/10.4161/cam.3.2.7767.
53. **Whitman MC, Fan W, Rela L, Rodriguez-Gil DJ, Greer CA.** 2009. Blood vessels form a migratory scaffold in the rostral migratory stream. J Comp Neurol **516:**94–104. http://dx.doi.org/10.1002/cne.22093.
54. **Bovetti S, Hsieh YC, Bovolin P, Perroteau I, Kazunori T, Puche AC.** 2007. Blood vessels form a scaffold for neuroblast migration in the adult olfactory bulb. J Neurosci **27:**5976–5980. http://dx.doi.org/10.1523/JNEUROSCI.0678-07.2007.
55. **Etienne-Manneville S, Hall A.** 2001. Integrin-mediated activation of Cdc42 controls cell polarity in migrating astrocytes through PKCzeta. Cell **106:**489–498. http://dx.doi.org/10.1016/S0092-8674(01)00471-8.
56. **Del Pozo MA, Kiosses WB, Alderson NB, Meller N, Hahn KM, Schwartz MA.** 2002. Integrins regulate GTP-Rac localized effector interactions through dissociation of Rho-GDI. Nat Cell Biol **4:**232–239. http://dx.doi.org/10.1038/ncb759.
57. **Kiosses WB, Shattil SJ, Pampori N, Schwartz MA.** 2001. Rac recruits high-affinity integrin alphavbeta3 to lamellipodia in endothelial cell migration. Nat Cell Biol **3:**316–320. http://dx.doi.org/10.1038/35060120.
58. **McCarty JH.** 2009. Cell adhesion and signaling networks in brain neurovascular units. Curr Opin Hematol **16:**209–214. http://dx.doi.org/10.1097/MOH.0b013e32832a07eb.
59. **Jannuzi AL, Bunch TA, West RF, Brower DL.** 2004. Identification of integrin beta subunit mutations that alter heterodimer function in situ. Mol Biol Cell **15:**3829–3840. http://dx.doi.org/10.1091/mbc.E04-02-0085.
60. **Sun T, Aceto N, Meerbrey KL, Kessler JD, Zhou C, Migliaccio I, Nguyen DX, Pavlova NN, Botero M, Huang J, Bernardi RJ, Schmitt E, Hu G, Li MZ, Dephoure N, Gygi SP, Rao M, Creighton CJ, Hilsenbeck**

SG, Shaw CA, Muzny D, Gibbs RA, Wheeler DA, Osborne CK, Schiff R, Bentires-Alj M, Elledge SJ, Westbrook TF. 2011. Activation of multiple proto-oncogenic tyrosine kinases in breast cancer via loss of the PTPN12 phosphatase. Cell **144:**703–718. http://dx.doi.org/10.1016/j.cell.2011.02.003.

61. **Kim Y, Comte I, Szabo G, Hockberger P, Szele FG.** 2009. Adult mouse subventricular zone stem and progenitor cells are sessile and epidermal growth factor receptor negatively regulates neuroblast migration. PLoS One **4:**e8122. http://dx.doi.org/10.1371/journal.pone.0008122.
62. **Lacy-Hulbert A, Smith AM, Tissire H, Barry M, Crowley D, Bronson RT, Roes JT, Savill JS, Hynes RO.** 2007. Ulcerative colitis and autoimmunity induced by loss of myeloid alphav integrins. Proc Natl Acad Sci U S A **104:**15823–15828. http://dx.doi.org/10.1073/pnas.0707421104.
63. **Travis MA, Reizis B, Melton AC, Masteller E, Tang Q, Proctor JM, Wang Y, Bernstein X, Huang X, Reichardt LF, Bluestone JA, Sheppard D.** 2007. Loss of integrin alpha(v)beta8 on dendritic cells causes autoimmunity and colitis in mice. Nature **449:**361–365. http://dx.doi.org/10.1038/nature06110.
64. **Shibahara K, Ota M, Horiguchi M, Yoshinaga K, Melamed J, Rifkin DB.** 2013. Production of gastrointestinal tumors in mice by modulating latent TGF-beta1 activation. Cancer Res **73:**459–468. http://dx.doi.org/10.1158/0008-5472.CAN-12-3141.
65. **Rhee I, Zhong MC, Reizis B, Cheong C, Veillette A.** 2014. Control of dendritic cell migration, T cell-dependent immunity, and autoimmunity by protein tyrosine phosphatase PTPN12 expressed in dendritic cells. Mol Cell Biol **34:**888–899. http://dx.doi.org/10.1128/MCB.01369-13.
66. **Jung Y, Kissil JL, McCarty JH.** 2011. Beta8 integrin and band 4.1B cooperatively regulate morphogenesis of the embryonic heart. Dev Dyn **240:**271–277. http://dx.doi.org/10.1002/dvdy.22513.
67. **Chang CC, Yang YJ, Li YJ, Chen ST, Lin BR, Wu TS, Lin SK, Kuo MY, Tan CT.** 2013. MicroRNA-17/20a functions to inhibit cell migration and can be used a prognostic marker in oral squamous cell carcinoma. Oral Oncol **49:**923–931. http://dx.doi.org/10.1016/j.oraloncology.2013.03.430.
68. **Hibbs K, Skubitz KM, Pambuccian SE, Casey RC, Burleson KM, Oegema TR, Jr, Thiele JJ, Grindle SM, Bliss RL, Skubitz AP.** 2004. Differential gene expression in ovarian carcinoma: identification of potential biomarkers. Am J Pathol **165:**397–414. http://dx.doi.org/10.1016/S0002-9440(10)63306-8.
69. **Hu X, Guo J, Zheng L, Li C, Zheng TM, Tanyi JL, Liang S, Benedetto C, Mitidieri M, Katsaros D, Zhao X, Zhang Y, Huang Q, Zhang L.** 2013. The heterochronic microRNA let-7 inhibits cell motility by regulating the genes in the actin cytoskeleton pathway in breast cancer. Mol Cancer Res **11:**240–250. http://dx.doi.org/10.1158/1541-7786.MCR-12-0432.
70. **Xu Z, Wu R.** 2012. Alteration in metastasis potential and gene expression in human lung cancer cell lines by ITGB8 silencing. Anat Rec **295:**1446–1454. http://dx.doi.org/10.1002/ar.22521.